Quantitative description of atomic architecture in solid solutions: A generalized theory for multicomponent short-range order

Anna V. Ceguerra,* Rebecca C. Powles, Michael P. Moody, and Simon P. Ringer†
Australian Centre for Microscopy & Microanalysis, The University of Sydney, New South Wales 2006, Australia
(Received 24 August 2010; published 11 October 2010)

This Brief Report introduces a short-range order parameter, called the generalized multicomponent short-range order (GM-SRO) parameter. The application to Monte Carlo simulations is described for higher order solid solutions. The results show the ability to create atomic-scale systems with a particular subset of the GM-SRO parameters and the power of the GM-SRO expressions in determining the relationship between two sets of atomic species.

DOI: 10.1103/PhysRevB.82.132201 PACS number(s): 61.66.Dk, 61.46.Bc, 61.72.sh

Sixty years ago Cowley proposed the definition of SRO as an approximate description of the distribution of solute atoms within the matrix of a binary alloy. This theory, known widely as the Warren-Cowley short-range order (WC-SRO) parameter, is defined by

$$\alpha_{BA}^{m} = 1 - p_{BA}^{m}/X_A, \tag{1}$$

where p_{BA}^{m} is the probability of finding an A-type matrix atom in the mth shell of atoms surrounding a B-type solute atom, given X_A the overall concentration of A atoms in the system. In the simplest case where $m=1$, this parameter describes the probability of finding a certain type of nearest-neighbor atomic bond in a binary alloy normalized against the nominal concentration.[1] The definition may be extended for progressively higher order crystallographic shells, measuring increasingly longer range order with increasing m. The concept of WC-SRO is an exceptional enabler in materials characterization for binary systems. Experimentally, x-ray diffraction techniques facilitate SRO measurements without knowledge of the exact positions of the atoms themselves, rather only the atoms' positions relative to each other.[2]

Unfortunately, after the experiment the calculations required to take advantage of the mathematical elegance of the WC-SRO definition above can be prohibitive. This is due to the technical infeasibility of stripping nonstructural information from the diffracted intensities in ternary and higher order systems although expressions up to quaternary systems do exist.[3] Hence, significant research has been directed toward generating an expression for multicomponent systems, including the use of Flinn operators,[4] multibody SRO,[5] and microchemical inhomogeneity.[6,7] Most notably, De Fontaine[8] extended the Warren-Cowley definition to what we refer to as the pairwise multicomponent short-range order (PM-SRO) parameter. The PM-SRO is defined as

$$\alpha_{BC}^{m} = \frac{p_{BC}^{m} - X_C}{\delta_{BC} - X_C}, \tag{2}$$

where δ_{BC} equals one if B=C and zero otherwise, and p_{BC}^{m} is the average probability of finding a C-type atom around a B-type atom. This parameter is not only pertinent for multicomponent systems (i.e., ternary and higher order systems) in that it examines pairs of atomic species; it also reduces to the WC-SRO parameter in binary systems. However, each PM-SRO parameter does not consider more than two atomic species at the same time, providing only an incomplete description of the system.

Nevertheless, PM-SRO is a powerful description of the shell-based relationships and has facilitated new approaches for predicting and measuring SRO in multicomponent systems. For example, using the calculation of phase diagrams (CALPHAD) (Ref. 9) set of tools to enable the prediction of phase diagrams from thermodynamic properties, Zhu *et al.*[10] derived an expression, based upon minimization of the Gibbs free-energy equation, for the atomic pairwise probabilities enabling an estimation of the system's PM-SRO values. This method does not simulate the atomic positions directly; rather, it is a numerical approach predicting the PM-SRO based on these equations, although a method exists where the WC-SRO is measured from a simulated system.[11] Alternatively, atom probe microscopy (APM) is emerging as a promising *experimental* approach for characterizing SRO. APM provides three-dimensional atomic scale spatial resolution combined with highly accurate chemical information.[12] Hence, it ought to be possible to derive PM-SRO relationships from measurements of the atomic positions revealed by APM.[13] Such methods would provide the means to predict and directly measure PM-SRO.

Here, we present a set of equations that provide a more holistic description of the SRO of a multicomponent system that is easier to interpret. Our generalized multicomponent short-range order (GM-SRO) considers two *sets* of atomic species for each coefficient, rather than just two individual atomic species for each parameter, where a positive GM-SRO indicates cosegregation. In this way, multiple species may be investigated for ordering or coclustering, in terms of the shell-based concentration. The GM-SRO incorporates probability terms comprised of a linear combination of PM-SRO probabilities. Based upon the principle of finding particular types of atoms around another atom, the GM-SRO probability term is derived as

$$p_{\{B_j\}_{j=1}^{k}\{B_l\}_{l=h}^{u}}^{m} = p_{\{B_1|\ldots|B_k\}\{B_h|\ldots|B_u\}}^{m} = \frac{\sum_{j=1}^{k} N_{B_j} \sum_{l=h}^{u} p_{B_jB_l}^{m}}{\sum_{j=1}^{k} N_{B_j}}. \tag{3}$$

This equation represents the probability of finding an atom of any of the one or more species—denoted by B_l—in the mth

shell around an atom of any of the species denoted by B_j. Given this expression for the GM-SRO probability term, the PM-SRO formula[8] can now be extended to consider two sets of multiple species at any particular mth shell

$$\alpha^m_{\{B_j\}_{j=1}^k\{B_l\}_{l=h}^u} = \alpha^m_{\{B_1|\ldots|B_k\}\{B_h|\ldots|B_u\}} = (-1)^{(1+\delta_{\{B_j\}_{j=1}^k\{B_l\}_{l=h}^u})}\left[\frac{p^m_{\{B_j\}_{j=1}^k\{B_l\}_{l=h}^u} - X_{\{B_l\}_{l=h}^u}}{\delta_{\{B_j\}_{j=1}^k\{B_l\}_{l=h}^u} - X_{\{B_l\}_{l=h}^u}}\right], \tag{4}$$

where $\delta_{\{B_j\}_{j=1}^k\{B_l\}_{l=h}^u}$ equals one if the two sets contain exactly the same atomic species and zero otherwise, and $X_{\{B_j\}_{j=1}^k} = X_{B_1} + \cdots + X_{B_k}$ is the combined concentration of the neighboring species. A simple example calculation is demonstrated in Fig. 1. In terms of the number of these parameters, whereas the number of PM-SRO equations is n^2 (the number of combinations of pairs of atomic species), the number of GM-SRO equations is the number of combinations of set B_j and set B_l together, or the number of combinations of set B_j squared, $[\Sigma_{j=1}^n \binom{n}{j}]^2$. Indeed the PM-SRO expressions form a subset of the GM-SRO, which is a more complete description of the system.

Having defined this metric for a quantitative characterization of the atomic architecture in a multicomponent solid where certain components may exhibit clustering or anticlustering, the derivation of expressions for the standard deviation complementary to each of the GM-SRO parameters is key to the interpretation of the analysis. It enables quantitative identification of significant SRO interactions, as compared to the distribution of atoms in random data sets or as compared to another system of interest. The GM-SRO standard deviation is based on the general propagation of error calculation,[14] the standard deviation of the concentration of atomistic data,[15] and the standard deviation of the PM-SRO probability. For both the PM-SRO and GM-SRO parameters, the variance, or standard deviation squared, can be written as

$$\sigma^2(\alpha^m_{\{B_j\}_{j=1}^k\{B_l\}_{l=h}^n}) = \left[\frac{\sigma(p^m_{\{B_j\}_{j=1}^k\{B_l\}_{l=h}^u})}{(\delta_{\{B_j\}_{j=1}^k\{B_l\}_{l=h}^u} - X_{\{B_l\}_{l=h}^u})}\right]^2 + \left[\frac{(p^m_{\{B_j\}_{j=1}^k\{B_l\}_{l=h}^u} - \delta_{\{B_j\}_{j=1}^k\{B_l\}_{l=h}^u})\sigma(X_{\{B_l\}_{l=h}^u})}{(\delta_{\{B_j\}_{j=1}^k\{B_l\}_{l=h}^u} - X_{\{B_l\}_{l=h}^u})^2}\right]^2 \tag{5}$$

where $\sigma^2(X_{\{B_l\}_{l=h}^u}) = X_{\{B_l\}_{l=h}^u}(1 - X_{\{B_l\}_{l=h}^u})/N$, and the variance of either the PM-SRO [Eq. (6)] or the GM-SRO [Eq. (7)] is used, depending on which SRO parameter is used. For the PM-SRO parameter, the variance of the probability term is

$$\sigma^2_{\text{PM-SRO}}(p_{B_jB_l}) = \frac{1}{N_{B_j}}\sum_{i=1}^{N_j}\left(\frac{n_{i,B_jB_l}}{c_{i,B_j}} - p_{B_jB_l}\right)^2 \tag{6}$$

and for the GM-SRO parameter, the variance in the probability term is

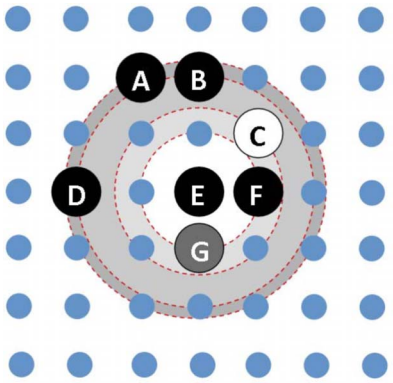

(a) Collate the individual probabilities, e.g. atom A has one out of its four neighbours as type Black.

i	$p_{\{Black\}\{x\}}(i)$
A, B	1/4 (x = Black)
D	0/4 (x = Black|Gray|White)
E, F	1/4 (x = Black)
E	1/4 (x = Gray)
F	1/4 (x = White)

(b) PM-SRO (first three rows) and GM-SRO (fourth) calculation

$\alpha_{\{B\}\{B\}}$	(4/20-5/49)/(44/49)
$\alpha_{\{B\}\{W\}}$	(1/20-1/49)/(-1/49)
$\alpha_{\{B\}\{G\}}$	(1/20-1/49)/(-1/49)
$\alpha_{\{B\}\{B\|G\|W\}}$	-(6/20-7/49)(-7/49)

FIG. 1. (Color online) PM-SRO and GM-SRO calculation for the first shell, for a quaternary system. The matrix atoms are in small and blue while the three solute atom types are labeled A–G. The first four shells are highlighted around solute atom E. The PM-SRO probabilities are first determined through collecting the probabilities for each atom, in this case in the first shell ($m=1$). Based on the PM-SRO probabilities, the GM-SRO probability is calculated, which is then used to generate the GM-SRO parameters.

$$\sigma^2_{\text{GM-SRO}}(p^m_{\{B_j\}_{j=1}^k\{B_l\}_{l=h}^u}) = \frac{1}{\sum_{j=1}^k N_{B_j}}\sum_{j=1}^k N_{B_j}\left[\sum_{l=h}^u \sigma(p_{B_jB_l})^2\right]. \tag{7}$$

The equations presented here can be applied to calculate the standard deviation of SRO when only a single data set is available. Calculation of the standard deviation enables quantitative identification of significant SRO interactions, as compared to the distribution of atoms in random data sets or as compared to another system of interest.

Having derived these expressions, the GM-SRO parameter is now demonstrated as applied to a model quaternary system. For the reasons identified above, there is limited PM-SRO experimental data describing multicomponent alloys available in the literature. Hence to determine the effective-

TABLE I. PM-SRO (Ref. 10) input to the Monte Carlo program. The reference atom type is i and j is the first shell nearest-neighbor type.

	j			
i	Al	Mg	Cu	Si
Al	6.4×10^{-3}	0.0	1.1×10^{-2}	1.1×10^{-2}
Mg	0.0	-2.7×10^{-3}	-1.0×10^{-1}	-1.2×10^{-1}
Cu	1.1×10^{-2}	-1.0×10^{-1}	7.5×10^{-3}	-3.3×10^{-1}
Si	1.1×10^{-2}	-1.6×10^{-1}	-3.3×10^{-1}	2.2×10^{-3}

ness of the GM-SRO equations derived above, we have chosen to simulate the atomic configuration that corresponds to a Al-1.75Cu-1.75 Mg-0.5Si (at. %) system defined by a set of PM-SRO values predicted by Zhu *et al.*[10] via CALPHAD calculations, as presented in Table I. Monte Carlo (MC) methods have previously been used to simulate systems with a particular SRO (Refs. 16 and 17) and these techniques offer insights into atomic structure that can be experimentally difficult to discover. Unlike the CALPHAD method, which does not provide atomic-scale information, the MC method recreates the system, enabling further nanostructural analysis and more intuitive interpretation offering insights that can be difficult to determine via experiments.

The approach developed in this study is based fundamentally on the previously outlined MC algorithm[16,17] for simulating a system with a target set of WC-SRO defined for multiple atomic shells. In this study PM-SRO definitions were incorporated into the algorithm since WC-SRO is restricted to binary systems and PM-SRO parameters are a subset of the GM-SRO. Indeed, the pairwise subset of the GM-SRO may also be used in lieu of the PM-SRO. A target atomic configuration is defined by a set of target PM-SRO, $\{\bar{\alpha}_{ik}^m\}_{1\le i,k\le n}$. Initially a distribution of atoms (most likely random) of an n-component system was simulated on the lattice with a corresponding set of PM-SRO parameters, $\{\alpha_{ik}^m\}_k$. At each step in the simulation, this method identifies the element within the set of current PM-SRO that is furthest from its corresponding target, i.e., the maximal ik pair: $\max\{|\alpha_{ik}^m-\bar{\alpha}_{ik}^m|\}_{1\le i,k\le n}$. A pair of atoms is chosen at random, based on this maximal ik pair, and their respective chemical identities are swapped. Swaps are accepted or rejected based upon the sum-squared residual,

$$\Delta_{\mathrm{SRO}}=\sum_{i=1}^{n}\sum_{k=1}^{n}[\alpha_{ik}^m-\bar{\alpha}_{ik}^m]^2,$$

estimated by calculating the overall residual in terms of the sum-squared differences between the target and the current recalculated PM-SRO. If Δ_{SRO} is decreased by the swap, the move is accepted; otherwise, the move may be rejected with respect to some user-defined probability, unrelated to the resulting change in SRO. Further, the simulation incorporates other features that were implemented such that the algorithm was optimized to maintain accuracy in the case of the simulation of small systems, yet efficient enough to generate very large systems with the prescribed PM-SRO within a reasonable time. This included: periodic boundary conditions, efficient calculation of Δ_{SRO} and an automatic restart/backtrack criterion to avoid the simulation becoming trapped in an imperfect configuration. The implemented program was run on a 16-core server with 32 GB of RAM, with 32 million atoms and for two different targets, that of PM-SRO=0 and the PM-SRO given in Table I. The first target reached the residual tolerance level of 10^{-6} in 1.36 million steps and 37 min, and the second target ran for 7.1 million steps in 2.1 h. The residual was in relative units.

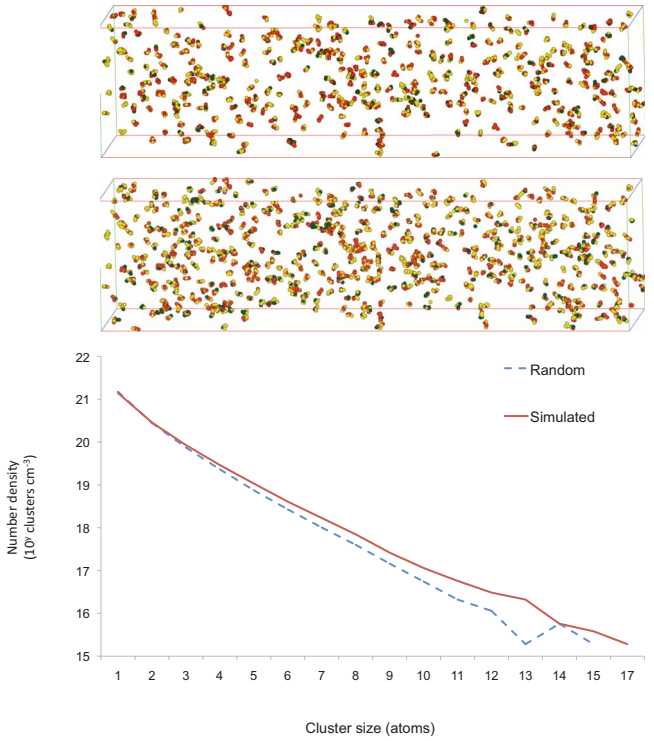

FIG. 2. (Color online) Clusters identified using the 3-dimensional Markov field (3DMF) algorithm of synthetic quaternary data (Al-1.75Cu-1.75Mg-0.05Si) with a volume of $20\times20\times80$ nm^3. Atom map for clusters containing five atoms or more in (a) random PM-SRO=0 data set and (b) with the PM-SRO in Table I. (c) Cluster size distribution comparison between simulated and random.

In comparison to the original random distribution, the effect of the applied PM-SRO values on the atomic configuration is subtle and hence difficult to ascertain visually. However, cluster-distribution analysis[13,18,19] highlights significant difference between the random and simulated data in terms of cluster size distribution as shown in Fig. 2. The analysis indicates more than expected solute clusters in the simulated system, implying that on average solute atoms are expected to be less likely to be found adjacent to one another. This cluster distribution underscores the delicate balance required in the atomic configuration required to meet all of the predefined PM-SRO components. Indeed cluster morphology analysis indicates the nanostructure is more likely to take on a lathelike form in the simulated data set in comparison to the random system.

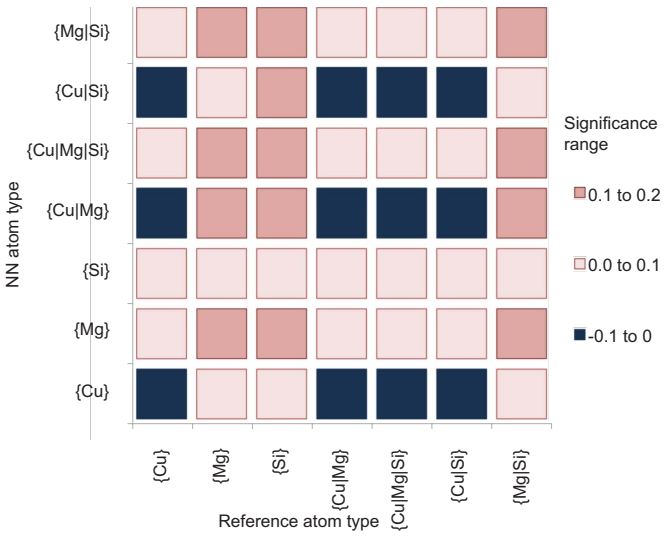

FIG. 3. (Color online) GM-SRO significance of the parameter compared to GM-SRO=0. The red shades indicate a GM-SRO that is greater than random and blue shades indicate a negative difference between simulated and random.

This point is underscored by the applied GM-SRO analysis, which provides a complete description of the solute-solute interactions in the simulated system, the significance values of which are presented in Fig. 3, where a positive significance indicates correlations. The GM-SRO provides a significant advance in ease of interpretation, when compared to the PM-SRO analysis given by Zhu *et al.*[10] Despite the differences in sign, the trends in cosegregation or antisegregation analysis remain the same as in this previous publication, for example, with respect to the $\alpha_{\{Cu\}\{Mg\}}$ and $\alpha_{\{Mg\}\{Si\}}$. Figure 3 confirms significant correlations between specific pairs of sets of solute species, as expected. For example, {Mg|Si} atoms which have any solute type combination as a first shell nearest-neighbor has higher GM-SRO than random. However, it is interesting that although {Cu} has positive PM-SRO with respect to both {Mg} and {Si}, GM-SRO indicates anticorrelations with the set of {Cu|Mg} and {Cu|Si}. Nevertheless, for the most part the GM-SRO indicates correlations between sets of atomic species. Such correlations between groups explain the increased incidence of solute clustering observed in the simulated system in Fig. 2. The results illustrate how the GM-SRO is necessary to complete the picture of the solute interactions within multicomponent alloys. Further, they are indicative of the fine balance that must be struck in the course of the MC simulation to create an atomic distribution that meets all of the target PM-SRO criteria.

In conclusion, the generalized multicomponent SRO provides a physical interpretation of the nanostructure of materials. It is a generalization of the pairwise multicomponent SRO equations, which in a binary system reduces to the Warren-Cowley SRO parameter, thus allowing the calculation of the GM-SRO parameters from the PM-SRO values. This parameter can identify more complex correlations between sets of atomic species, in a way that is not apparent using the PM-SRO, and that is simpler to interpret. A Monte Carlo algorithm provides the means to simulate a system with a particular set of PM-SRO parameters with reasonable time and memory requirements even for very large data sets. These methods enable the investigation of nanoscale phenomena such as solute clustering in a way that was not possible with PM-SRO predictions alone. There are two caveats to the GM-SRO measure. First, the GM-SRO parameter is not a unique identifier of a system rather, it summarizes the atomic-scale relationships with respect to the random shell concentration, making it a high-level descriptor. Thus, multiple chemical configurations are possible given a particular set of GM-SRO parameters. Second, the interpretation of the GM-SRO is as straightforward as reading a negative GM-SRO parameter as being indicative of a system with fewer clusters than random for those sets of atomic species; similarly the positive GM-SRO parameter indicates more clusters. In fact, as this particular study shows, the complete GM-SRO parameters depict a fine balance in the chemical configuration of the atomic scale data.

The authors are grateful for scientific and technical support from the Australian Microscopy & Microanalysis Research Facility (AMMRF) node at the University of Sydney (ACMM), particularly Tim Petersen, Leigh Stephenson, and Daniel Haley. A.C. acknowledges support from the Australian Government, the University of Sydney, and CSIRO.

*anna.ceguerra@sydney.edu.au
†simon.ringer@sydney.edu.au

[1] J. M. Cowley, Phys. Rev. **77**, 669 (1950).
[2] J. M. Cowley, J. Appl. Phys. **21**, 24 (1950).
[3] G. B. Taggart, Phys. Rev. B **19**, 3230 (1979).
[4] G. B. Taggart, J. Phys. Chem. Solids **34**, 1917 (1973).
[5] G. B. Taggart and R. A. Tahir-Kheli, Prog. Theor. Phys. **47**, 370 (1972).
[6] J. H. Li *et al.*, J. Phys. Chem. B **108**, 16071 (2004).
[7] J. H. Li *et al.*, Phys. Rev. B **69**, 172201 (2004).
[8] D. de Fontaine, J. Appl. Crystallogr. **4**, 15 (1971).
[9] N. Saunders and A. P. Miodownik, *CALPHAD (Calculation of Phase Diagrams): A Comprehensive Guide* (Pergamon, Oxford, 1998).
[10] A. Zhu *et al.*, Acta Mater. **52**, 3671 (2004).
[11] M. Slabanja *et al.*, Surf. Interface Anal. **39**, 178 (2007).
[12] D. N. Seidman and K. Stiller, MRS Bull. **34**, 717 (2009).
[13] A. V. Ceguerra *et al.*, Philos. Mag. **90**, 1657 (2010).
[14] J. R. Taylor, *An Introduction to Error Analysis* (University Science Books, Sausalito, CA 1997).
[15] M. K. Miller *et al.*, *Atom Probe Field Ion Microscopy* (Oxford Science, New York, 1996).
[16] P. C. Gehlen and J. B. Cohen, Phys. Rev. **139**, A844 (1965).
[17] V. Gerold and J. Kern, Acta Metall. **35**, 393 (1987).
[18] J. M. Hyde and C. A. English, in *Symposium R: Microstructural Processes in Irradiated Materials*, MRS 2000 Fall Meeting Vol. 650 (Materials Research Society, Boston, MA, 2000), p. R6.6.1.
[19] L. T. Stephenson *et al.*, Microsc. Microanal. **13**, 448 (2007).